

A substellar component orbiting the F-star 30 Arietis B^{★,★★}

E. W. Guenther^{1,★★★}, M. Hartmann¹, M. Esposito², A. P. Hatzes¹, F. Cusano¹, and D. Gandolfi¹

¹ Thüringer Landessternwarte Tautenburg, Sternwarte 5, 07778 Tautenburg, Germany
e-mail: guenther@tls-tautenburg.de

² Hamburger Sternwarte, Gojenbergsweg 112, 21029 Hamburg, Germany

Received 19 March 2009 / Accepted 14 September 2009

ABSTRACT

Context. Most current radial velocity planet search programs have concentrated on stars of one solar mass. Our knowledge on the frequency of giant planets and brown dwarf companions to more massive stars is thus rather limited. In the case of solar-like stars, the frequency of short-period brown dwarf companions and very massive planets seems to be low.

Aims. Here we present evidence for a substellar companion to 30 Ari B, an F-star of $1.16 \pm 0.04 M_{\odot}$ that is a member of a hierarchical triple system.

Methods. The companion was detected by means of precise radial velocity measurements using the 2-m Alfred-Jensch telescope and its échelle spectrograph. An iodine absorption cell provided the wavelength reference for precise stellar radial velocity measurements.

Results. We analyzed our radial velocity measurements and derived an orbit to the companion with period, $P = 335.1 \pm 2.5$ days, eccentricity $e = 0.289 \pm 0.092$, and mass function $f(m) = (6.1 \pm 1.7) \times 10^{-7} M_{\odot}$.

Conclusions. We conclude that the radial velocity variations of 30 Ari B are due to a companion with $m \sin i$ of $9.88 \pm 0.94 M_{\text{Jup}}$ that is either a massive planet or a brown dwarf. The object thus belongs to the rare class of massive planets and brown dwarfs orbiting main-sequence stars.

Key words. stars: individual: 30 Arietis B – stars: low-mass, brown dwarfs – planetary systems – techniques: radial velocities

1. Introduction

Although the mass of the host star is likely to be important for planet formation, our knowledge of the dependence between the mass of the host star and the frequency and mass of planets is still rather limited (Udry & Santos 2007). This is, because most planet search programs focus on dwarfs of about one solar mass, or less.

Although there is strong evidence that stars less massive than the sun have a lower frequency of giant planets, it still has not been observationally established whether a different frequency of giant planets holds for stars more massive than the sun. A correlation between the mass of the planets, and the host stars is expected because the mass of the proto-planetary disk scales with the mass of the stars (Lovis & Mayor 2007). Radial velocity searches for planets around more massive, early-type main-sequence stars are problematical due to the paucity of lines and often rapid rates of rotation – the RV precision is often inadequate for the detection of substellar companions. In spite of these difficulties a few searches have been conducted. Galland et al. (2005a) surveyed a sample of A–F stars and discovered a planetary candidate in a 388-day orbit with $m \sin i = 9.1 M_{\text{Jup}}$ around the F6V star HD 33564 which has a mass of $1.25^{+0.03}_{-0.04} M_{\odot}$ (Galland et al. 2005b). They also found a brown dwarf candidate with $m \sin i = 25 M_{\text{Jup}}$ in a 28-day orbit around the A9V star HD 180777 (Galland et al. 2006).

* Based on observations obtained at the 2-m Alfred-Jensch telescope at the Thüringer Landessternwarte Tautenburg.

** Table 3 is only available in electronic form at the CDS via anonymous ftp to cdsarc.u-strasbg.fr (130.79.128.5) or via <http://cdsweb.u-strasbg.fr/cgi-bin/qcat?J/A+A/507/1659>

*** Visitor at the Instituto de Astrofísica de Canarias, C/ Vía Láctea, s/n, 38205 La Laguna (Tenerife), Spain.

An alternative approach is to conduct RV searches for those early-type main-sequence stars that have evolved onto the giant branch. The cool effective temperatures and slow rotation rates make these stars much more amenable to RV searches even if the mass determination is more problematical for such stars. Currently about 20 giant planets have been found around giant stars in the mass range of 1.1–2.5 M_{\odot} (e.g. Frink et al. 2002; Sato et al. 2003; Setiawan et al. 2005; Döllinger et al. 2007; Lovis & Mayor 2007; Sato et al. 2007). These planets tend to have masses in the range of 3–10 M_{Jup} hinting that more massive stars tend to have more massive planets. Interestingly, the well known relation between metallicity and planet frequency for solar-like stars is less pronounced in giant stars (Schuler et al. 2005). Pasquini et al. (2007) argued that the planet-metallicity effect may be a result of atmospheric pollution caused by migrating planets being swallowed up by the star. In giant stars there is also a lack of planets with semi-major axis of ≤ 0.6 AU and possibly also a different distribution of the eccentricities. Sato et al. (2007) discuss whether the lack of close-in planets in giant stars is due to a difference in the formation of planets of more massive star, or due to the fact that planets moves outwards when the central stars loose mass, or whether the inner planets are engulfement by their host stars when these expand. The discovery of the planet of the sdB star V391 Peg is very interesting in this respect as this planet must have survived the red-giant phase, when the star expanded to 70% of the star-planet distance (Silvotti et al. 2007; Fortney 2007). Once a sufficient number of planets of giant and main-sequence stars that are more massive than the sun are found, it will be possible to find out whether the lack of planets with 0.6 AU in giant stars is due to the formation, or evolution of the planets. If it were due to formation, we would find the same lack of inner planets in main-sequence stars more massive than the sun as in giant stars.

According to the theory by Kennedy & Kenyon (2008), the probability that a given star has at least one gas giant planet increases linearly with stellar mass from 0.4 to $3 M_{\odot}$. Kornet et al. (2006) concluded that giant planets tend to form in tighter orbits around *less* massive stars. Although they find that the minimum metallicity at which planets can form via core accretion decreases with increasing mass of the central star, they also conclude that the frequency of massive planets should be anticorrelated with the mass of the star.

Searching for planets around main-sequence stars more massive than the sun is possible if one restricts the search to stars in the range between 1.1 to about $1.7 M_{\odot}$ (F-stars) and on the detection of massive planets. Such stars have still enough spectral lines and the rotation rates are still modest compared to more massive stars so that a reasonable RV precision is achieved. Additionally, the mass of the convection zone of F-stars is a factor 10 smaller than that of K stars allowing us to investigate the atmospheric pollution hypothesis as well (Pinsonneault et al. 2001).

In here we report on the indirect detection of a massive planet around the F6V star 30 Ari B, which is also part of a hierarchical triple system.

2. The host star 30 Ari B

30 Ari is a visual binary star with a separation of 38.2 ± 0.7 arcsec (Shatsky 2001) consisting of the components 30 Ari A (HD 16246, HIP 12189) and 30 Ari B (HD 16232, HIP 12184). 30 Ari A is a single line spectroscopic binary. Morbey & Brosterhus (1974) derive an orbital period of 1.109526 ± 0.000001 days, an eccentricity of 0.062 ± 0.012 , and an amplitude of 22.41 ± 0.31 km s⁻¹. Using the Hipparcos parallax of the two stars (Perryman et al. 1997; Zombeck 2006) the distance to 30 Ari A, B is 39.8 ± 0.3 pc, which yields a projected distance between the two stars of about 1520 ± 54 AU. The orbital period thus is likely to be larger than 10000 years. As expected for a close binary system, 30 Ari A is an X-ray source and was detected by ROSAT with an X-ray flux of 0.472 ± 0.046 ct/s (Zickgraf et al. 2003). 30 Ari B was not detected by ROSAT.

30 Ari A is listed in the SIMBAD database with a spectral type F6III. If true, the object should have an absolute brightness (M_v) of +1.4 mag. Using again the Hipparcos distance, the relative magnitude (m_v) would than be 4.4 mag, which is inconsistent with the observed brightness (Table 1). The $V - J$ colours are 0.808 ± 0.02 for 30 Ari A and 1.02 ± 0.02 for 30 Ari B, and the $V - K$ colours are 1.01 ± 0.3 and 1.27 ± 0.02 for components A and B, respectively. The colours are also inconsistent with a giant star but consistent with a main-sequence star. Using our high resolution spectra (see Sect. 3) and following the method described in Frasca et al. (2003) and Gandolfi et al. (2008), we find that 30 Ari A is an F5V star and 30 Ari B, and 30 Ari B and F6V star (Figs. 1; 2). Thus, the brightness, colours and the results of the spectroscopy show that both components are still on the main sequence stars.

Figure 3 shows the position of both stars in the Hertzsprung-Russell diagram, together with the evolutionary tracks from Girardi et al. (2000). Averaging the stellar parameters and the using the method described in da Silva et al. (2006), we derive the age, masses, and diameters of the two stars (Table 1). We find that the mass of 30 Ari A and B are 1.31 ± 0.04 and $1.16 \pm 0.04 M_{\odot}$, respectively. For the ages of the two stars we derive 0.86 ± 0.63 and 0.91 ± 0.83 Gyr. The $v \sin i$ values are also typical for stars of that age and spectral type. The basic stellar

Table 1. Stellar properties of 30 Ari A, B.

Parameter	30 Ari A	30 Ari B
RA	02 37 00.5237	02 36 57.7405
Dec	+24 38 50.0000	+24 38 53.0270
Spectral type	F5V ¹⁴	F4V ⁴ , F6V ⁶ , F6V ¹⁴
$v \sin i$ [km s ⁻¹]	38.5 ± 2.6 ¹⁴	40.6 ⁷ , 38.3 ± 1.8 ¹⁴
V [mag]	6.497 ¹⁰ , 6.48 ⁵	7.091 ¹⁰ , 7.1 ⁵
$B - V$ [mag]	0.410 ^{8,13}	0.510 ^{12,13}
J [mag]	5.681 ± 0.019 ¹¹	6.080 ± 0.020 ¹¹
H [mag]	5.580 ± 0.051 ¹¹	5.908 ± 0.029 ¹¹
K [mag]	5.479 ± 0.024 ¹¹	5.822 ± 0.021 ¹¹
M_v	3.48 ¹⁰ , 3.46 ⁵	4.12 ¹⁰ , 4.12 ⁵
π [mas]	24.92 ± 1.05 ³	25.36 ± 1.10 ³
Distance [pc]	40.1 ± 1.7	39.4 ± 1.7
[Fe/H] [dex]	0.27 ⁴ , 0.00 ¹⁰ , 0.11 ²	0.27 ^{1,7} , -0.13 ¹⁰ , 0.245 ± 0.195 ⁹ , 0.03 ² , 0.27 ⁶
T_{eff} [K]	6462 ⁴ , 6668 ¹⁰ 6300 ± 60 ⁹ , 6726 ² 6457 ⁵	6462 ^{1,4} , 6152 ¹⁰ 6300 ± 60 ⁹ , 6364 ² , 6607 ⁵
$\log g$	4.51 ² , 4.25 ⁵	4.50 ⁴ , 4.54 ² , 4.44 ⁵
M_* [M_{\odot}]	1.32 ± 0.05 ¹⁰ , 1.36 ⁵ 1.31 ± 0.04 ¹⁴	1.11 ± 0.06 ¹⁰ , 1.20 ⁵ 1.16 ± 0.04 ¹⁴
Age [Gyr]	0.86 ± 0.63 ¹⁴	0.91 ± 0.83 ¹⁴
R_* [R_{\odot}]	1.37 ± 0.03 ¹⁰	1.13 ± 0.03 ¹⁴
θ [mas]	0.32 ± 0.01 ¹⁴	0.26 ± 0.01 ¹⁴

¹ Boesgaard & Friel (1990). ² Marsakov et al. (1995). ³ Hipparcos, Perryman & ESA (1997). ⁴ Cayrel de Strobel et al. (1997). ⁵ Allende Prieto et al. (1999). ⁶ Malagnini et al. (2000). ⁷ Buzzoni et al. (2001). ⁸ De Medeiros et al. (2002). ⁹ Taylor (2003). ¹⁰ Nordström et al. (2004). ¹¹ Skrutskie et al. (2006). ¹² Tolbert (1964). ¹³ Mermilliod (1991). ¹⁴ This work.

data are summarized in Table 1. As can be seen from the various abundance determinations both 30 Ari A and 30 Ari B are slightly metal rich.

3. Observations

30 Ari B was one of the stars monitored as part of the RV planet search program of the Thüringer Landessternwarte as described by Hatzes et al. (2005). For this program we used the 2-m-Alfred Jensch telescope of the Thüringer Landessternwarte Tautenburg which is equipped with an échelle spectrograph with resolving power of $\lambda/\Delta\lambda = 67\,000$. During the observations an iodine absorption cell was placed in the optical path in front of the spectrograph slit. The resulting iodine absorption spectrum that was superposed on top of the stellar spectrum provided a stable wavelength reference for the measurement of the stellar RV. All spectral observations were bias-subtracted, flat-fielded, and the échelle orders extracted using standard IRAF routines.

4. Radial velocity measurements and orbit of the companion

The RVs were calculated by modelling the observed spectra with a high signal-to-noise ratio template of the star (without iodine) and a scan of our iodine cell taken at very high resolution with the Fourier Transform Spectrometer of the McMath-Pierce telescope at Kitt Peak. The latter enables us to compute the relative velocity shift between stellar and iodine absorption lines as well as to model the temporal and spatial variations of the instrumental profile. See Valenti et al. (1995) and Butler et al. (1996) for a

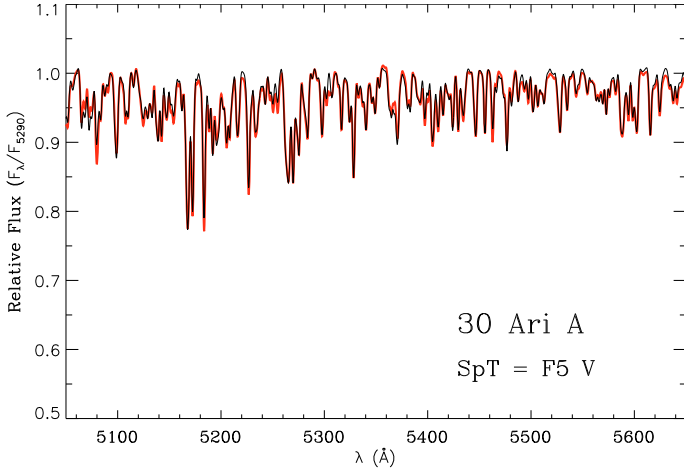


Fig. 1. Part of the TLS spectra of 30 Ari A. The observed spectra are displayed with thin lines, while the best fitting F5V templates are overplotted with thick lines. The spectra have been arbitrarily normalized to the flux at 5290 Å.

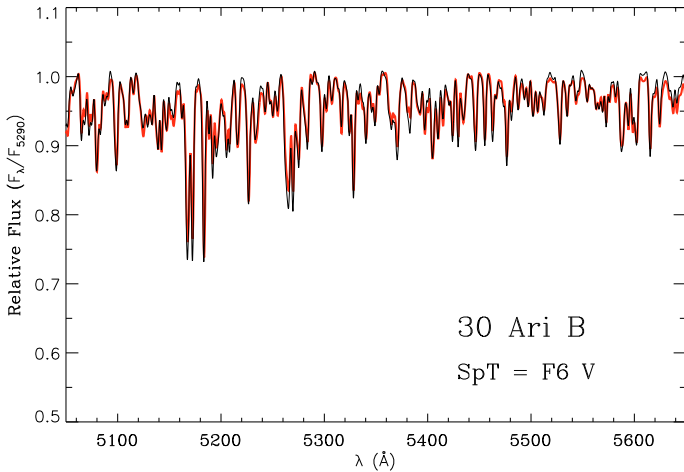


Fig. 2. Same as Fig. 1 but for 30 Ari B. The best fitting template is an F6V star.

description of the principles behind this technique. The median of the errors of the RV measurements for our planet program stars is about 9 m s^{-1} and 11% of these stars show RV variations of $\leq 6 \text{ m s}^{-1}$. This is based on the rms RV scatter for all stars with trends or orbital solutions removed (when companions are found). This error is mostly due to the S/N-ratio of the spectra and not to the inherent accuracy of the instrument, since we can achieve a precision of $\approx 3 \text{ m s}^{-1}$ on bright, slowly rotating late-type stars. However, for F-stars the accuracy is much lower, because of the fewer spectral lines. Since 30 Ari B is an F-star and rapidly rotating ($v \sin i 38.3 \pm 1.8 \text{ km s}^{-1}$), and since average S/N-ratio of the spectra is only 64 ± 20 , it is not surprising that the errors of each individual measurement is very large. As usual the errors of the measurements are derived from the standard-deviation of the RV values determined for each of the ~ 116 chunks into which the spectrum is divided (Endl et al. 2004; Hatzes et al. 2005, 2006; Döllinger et al. 2007, 2009). The median RV error for 30 Ari B is 152 m s^{-1} . Table 3 lists our RV measurements for 30 Ari B.

Figure 4 shows a periodogram of the data obtained since August 2002. There is only one significant peak at a frequency of 0.003 days^{-1} . For clarity, we also show a magnified version of this plot in Fig. 5. This peak is statistically significant. The false

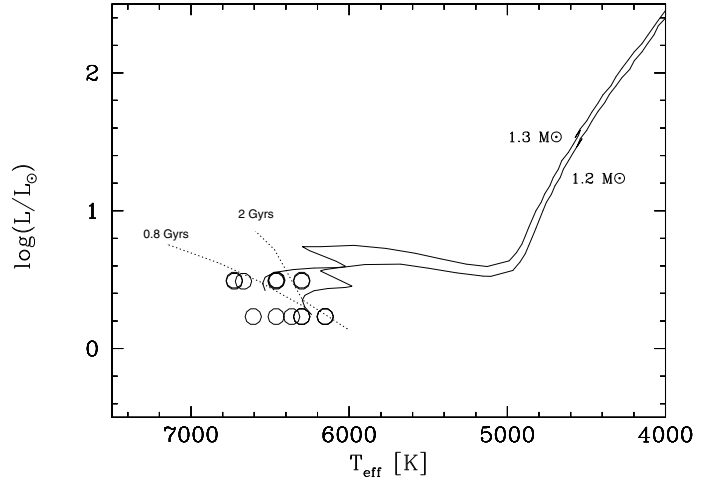


Fig. 3. The position of 30 Ari A and 30 Ari B in the Hertzsprung-Russell diagram, together with the evolutionary tracks from zero-age main-sequence stars to giant stars published by Girardi et al. (2000). The open circles show all values given in Table 1 for 30 Ari A. The filled circles correspond to 30 Ari B. The tracks are for masses of $1.2 M_{\odot}$ and $1.3 M_{\odot}$, and the isochrones for 0.8 and 2 Gyr from that article. Using the method described in da Silva et al. (2006), we derive the parameters given in Table 1.

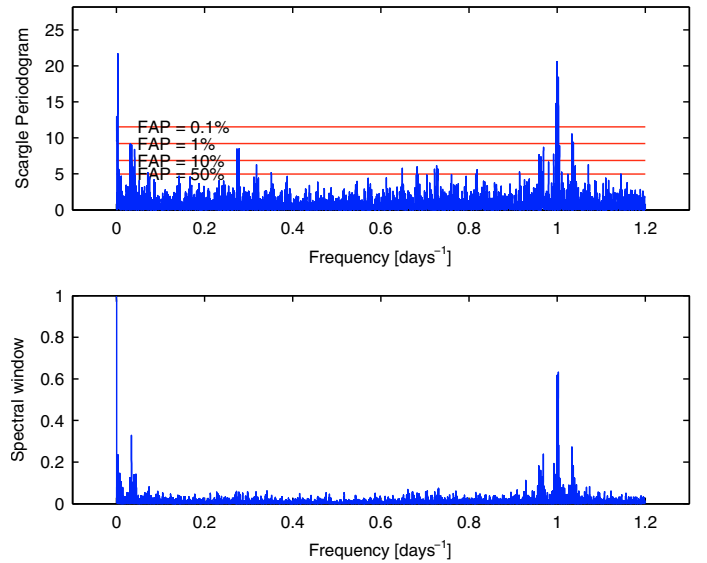


Fig. 4. Periodogram of the RV values. Apart from a one day alias, there is only one peak at a frequency of 0.003 days^{-1} . In the upper panel, the false alarm probability is added.

alarm probability (FAP) from the Lomb-Scargle periodogram alone yields $\approx 10^{-7}$. The FAP was also estimated using a bootstrap randomization technique. The measured RV values were randomly shuffled keeping the observed times fixed and a periodogram for each of these “random” data sets was then computed. The fraction of the random periodograms having power higher than the data periodogram yielded the false alarm probability that noise would create the detected signal. After 2×10^5 “shuffles” there was no instance where the random data periodogram had power higher than the real periodogram. This confirms the low value of the FAP.

The orbital solution was determined using the non-linear least squares fitting program *Gaussfit* (Jefferys et al. 1988). These orbital parameters are listed in Table 2. Figure 10 shows

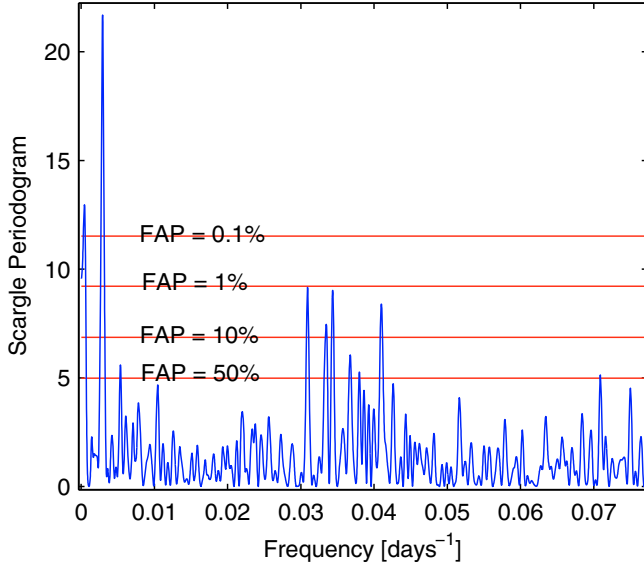


Fig. 5. Magnified periodogram close to the frequency of 0.003 days^{-1} (Fig. 4) showing that there is only one significant peak.

Table 2. Orbital elements of 30 Ari B.

Element	Value
Period [days]	335.1 ± 2.5
T_0 [HJD]	$245\,4538 \pm 20$
K_1 [m s^{-1}]	272 ± 24
e	0.289 ± 0.092
ω [deg]	307 ± 18
σ (O-C) [m s^{-1}]	135
$f(m) = \frac{m_2^3 \sin^3 i}{(m_1 + m_2)^2} [M_\odot]$	$(6.1 \pm 1.7) \times 10^{-7}$
$a_1 \sin i$ [AU]	0.00802 ± 0.00074
a [AU]	0.995 ± 0.012
$m_1 [M_\odot]$	1.16 ± 0.04
$m_2 \sin i [M_{\text{Jup}}]$	9.88 ± 0.94

the periodogram of the RV residuals after subtracting the orbital solution. There is no indication of additional signals (companions) in the RV data.

The classical Lomb-Scargle periodogram analysis is less than ideal for detecting planets in eccentric orbits. A better way to detect these is to phase-fold the data to all possible periods within a certain range and then fitting a Kepler orbit to the data for each period. As a test we also fitted all possible Kepler orbits with periods between less than one day and 2213 days, the time for which we monitored the object. We also varied the eccentricity between 0 and 0.9. The best orbital solution is the one that minimizes the variance between it and the RV measurements. Thus, $1/\text{variance}$ is maximized and this can be used as a measure of the quality of the fit. A high value of $1/\text{variance}$ indicates a small difference between the best Kepler orbit and the data. As can easily be seen in Figs. 8 and 9 the Kepler orbit which matches best the observed data has a period of 335 days. The parameters of the corresponding orbit are consistent with the *Gaussfit* solution, which is shown as a line in Fig. 7. The values derived given in Table 2. With a stellar mass of $1.16 \pm 0.04 M_\odot$, the minimum companion mass is $9.88 \pm 0.94 M_{\text{Jup}}$.

Unfortunately, the orbital period is close to one year which makes it difficult to cover all phases. Because of the relatively high latitude of Tautenburg observatory (+51 degrees) managed, however to obtain RV measurements of consecutive minima and maxima of the RV curve (Fig. 6). Further tests are nevertheless

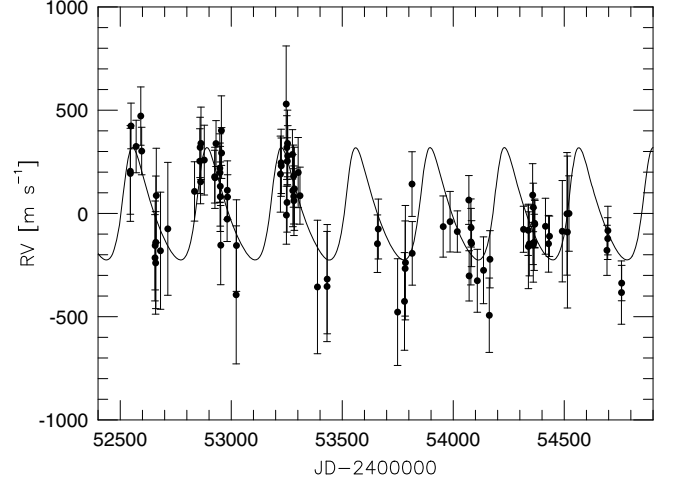


Fig. 6. RV measurements of 30 Ari B. The solid line is the orbital solution.

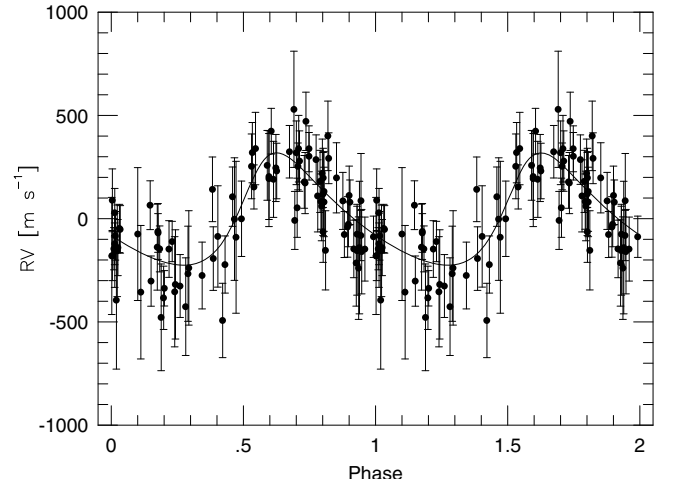


Fig. 7. Phase-folded RV curve together with the orbit.

required in order to find out whether this period is in fact a one year alias, or not. To test this hypothesis we permuted randomly the order of the RV measurements in respect to the time when the observations were taken, and applied the same period finding algorithm as before. If the period were due to an alias we should find the same period in the permuted as in the original data. The second line in Fig. 8 shows the periodogram just for one such permuted data set. We repeated the same experiment with 2×10^5 different permutations and none of these showed any significant peak in that period range.

Furthermore, the orbital period differs by more than 5 sigma from a 1-year period (Fig. 8). This excludes that the signal is an artifact of incomplete removal of the earth's barycentric motion. We thus conclude that the 335-day period in the RVs is real. Figure 6 shows the RV measurements together with the orbit and Fig. 7 the phase-folded RV measurements.

5. Activity or companion?

We find RV variations of 30 Ari B with a period of 335.1 ± 2.5 days. What is the nature of the RV variations? It is unlikely that this period is due to oscillations as such long-period pulsations have never been found in main-sequence stars. From the radius of $1.13 \pm 0.03 R_\odot$, and the $v \sin i$ of the star we derive that the rotation period has to be ≤ 1.5 days. It is thus impossible that

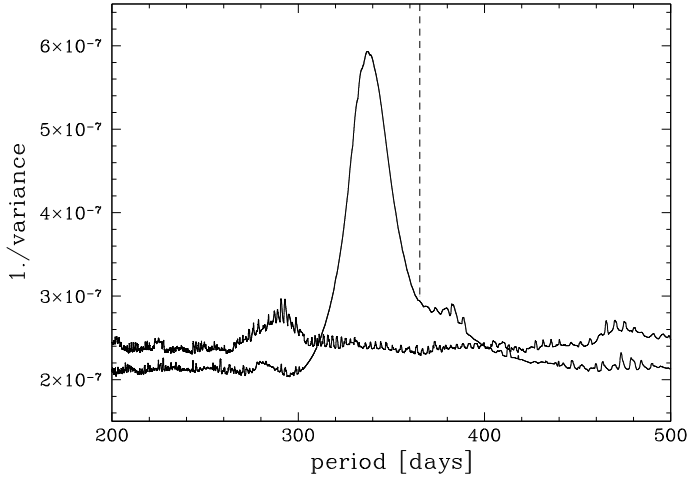


Fig. 8. Shown are the $1/\text{variance}$ of residuals between the RV measurements and the best-fitting Kepler orbit for a given period. The peak indicates that the difference between a Kepler orbit and the measurements is minimal for a period of 335 days, clearly different from one year (vertical dashed line). Also shown is $1/\text{variance}$ for just one of the permuted data sets demonstrating that there is no alias close to the 335-day period.

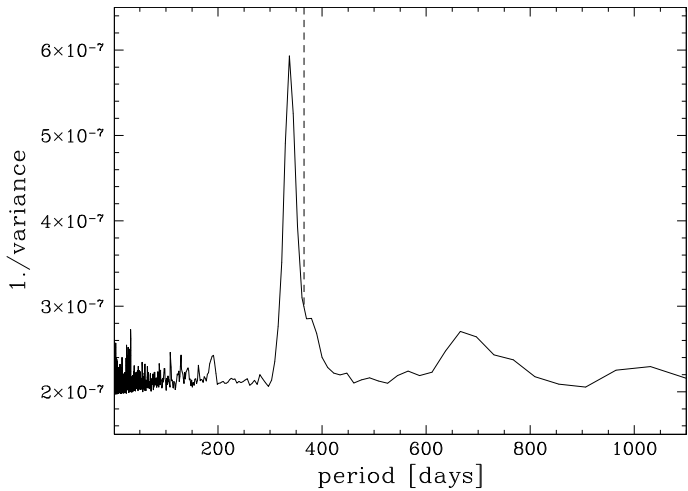


Fig. 9. Same as Fig. 8 but for the period range between 1.0 and 1100 days demonstrating that the largest peak is at a period of 335 days.

335 days is the rotation period of the star. In principle, another possibility would be that the RV variations are caused by an activity cycle. Variations on long time scales might be caused by changes of the granulation, which not only effects the RV but also the central depth and thus the equivalent width of photospheric lines (Livingston et al. 2007).

According to Ossendrijver (1997) the length of the activity cycle is given by the relation: $P_{\text{cyc}} = 6.9 P_{\text{rot}}^{2\pm 0.3} \tau_c^{-2\pm 0.3}$ [yrs], with the convective turnover time τ_c . The convective turnover time would thus have to be of the order of four days in order to explain an activity cycle P_{cyc} of 0.92 years. A τ_c of four days is certainly not very plausible for an F6V star (Ossendrijver 1997).

From the relationship between the filling factor and the RV jitter from Saar & Donahue (1997), we derive that the brightness of the star would have to change by $\geq 1\%$ if the observed RV variations were caused by spots. In order to test this hypothesis, we examined the photometric measurements taken with the Hipparcos satellite (Perryman & ESA 1997). Figure 11 shows the periodogram of the Hipparcos photometry and Fig. 12 the

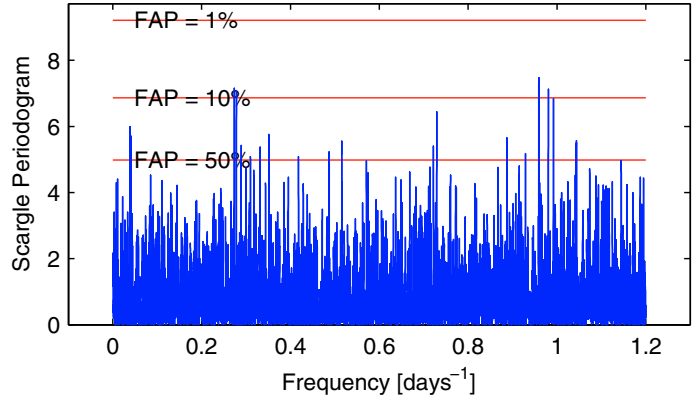


Fig. 10. Periodogram of the residuals of the RV after subtracting the orbit: There is no indication for another companion.

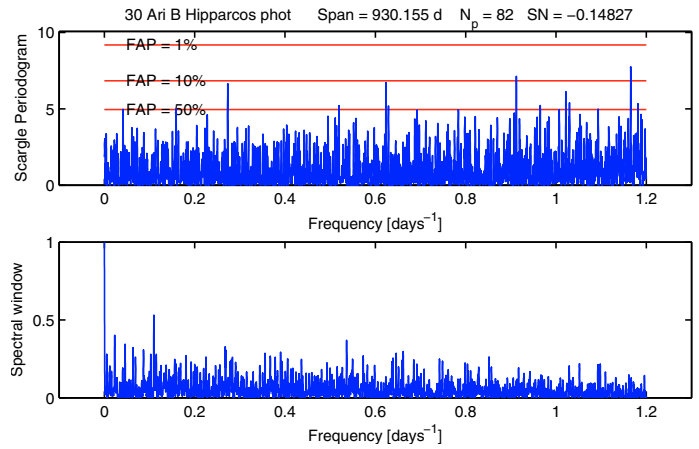


Fig. 11. Periodogram of the Hipparcos photometry. There is no peak at a frequency of 0.003 days^{-1} .

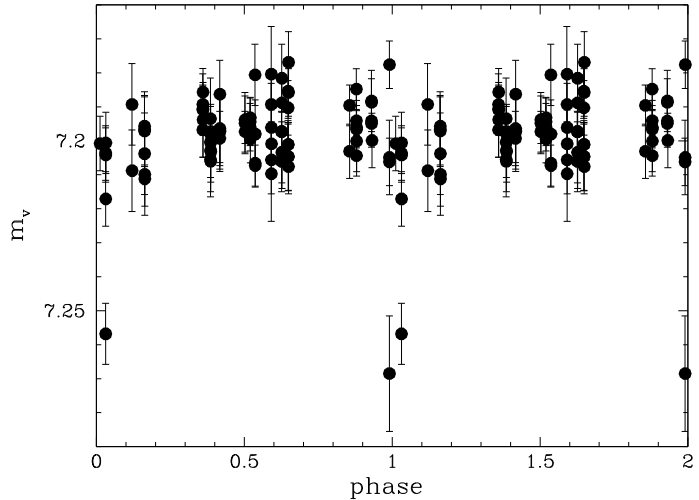


Fig. 12. Shown are photometric measurements taken with the Hipparcos satellite of 30 Ari B, phase-folded to the same period as in Fig. 7. The brightness of the star does not vary in phase with the RV.

values phase-folded to the orbital period given in Table 2. The photometric measurements do not show any periodicity associated with the planet period. We should note, however, that the Hipparcos photometry was not contemporaneous with our RV measurements. The average brightness of star in the interval of ± 0.1 in phase around the maximum and minimum of the RV is

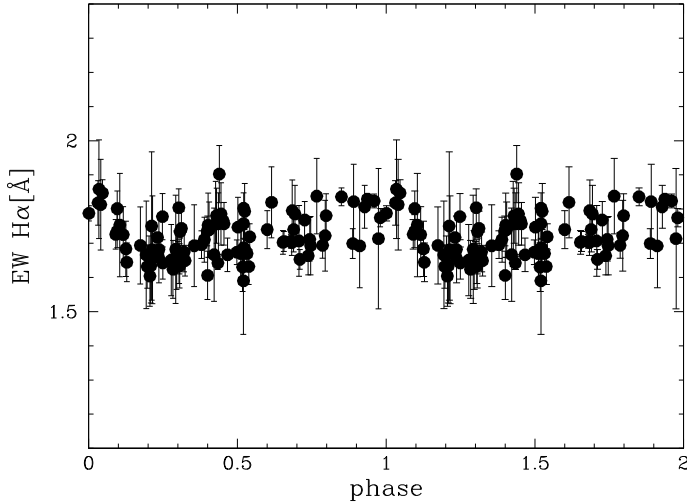


Fig. 13. Shown are measurements of the equivalent width of $H\alpha$ phase-folded to the same period as in Fig. 7. The equivalent width does not vary in phase with the RV.

7.1964 ± 0.0015 , and 7.1969 ± 0.0015 mag, respectively. Thus, the star has the same brightness at both phases which implies that there is no correlation between the brightness of the star and the RV.

As an additional test, we analyzed the strength of the $H\alpha$ and $H\beta$ lines. If we would find that the equivalent width, or the depth of $H\alpha$ and $H\beta$ were correlated with the RV, we would have to conclude that the RV variations are caused by stellar activity (König et al. 2005). Figure 13 shows the equivalent width measurements of $H\alpha$ phase-folded in the same way as Fig. 7. Even after binning the data in phase, we do not see any obvious variations that are in phase with the RV measurements. The equivalent width of $H\alpha$ variability is not correlated with the RV.

As another test, we averaged all spectra in the RV intervals $RV < -200$, $-200 < RV < 0$, $0 < RV < 200$, and $RV > 200$ m s^{-1} , and then divided these four spectra by the average of all spectra. The result is shown in Fig. 14 for the spectral region containing $H\beta$. Again, there is no evidence that the depth of $H\beta$ is correlated with the RV.

As a final test we did the same analysis for the photospheric lines. Unfortunately, the number of photospheric lines that are not affected by the iodine lines are rather limited. Figure 15 shows the averaged equivalent width of photospheric lines that are not affected by the iodine lines versus the RV. As before, we binned the data into velocity intervals. Again, there is no correlation between the equivalent width and the radial velocity. Since all four tests show no indication that the RV variations are caused by stellar activity, we conclude that they are caused by a companion.

6. Discussion and conclusions

We took RV measurements of the F-star 30 Ari B over a time span of six years. The RV shows periodic variations with a period of 335.1 ± 2.5 days, which can be fitted with a Keplerian orbit with an eccentricity of 0.289 ± 0.092 . Since the period remained unchanged during this time, and since the star shows neither significant photometric variations, nor significant variations of the Balmer, or photospheric lines, the best interpretation is that the RV variations are caused by an orbiting body.

This star is part of a hierarchical triple system. However, the large separation between 30 Ari A and 30 Ari B (about 1500 AU)

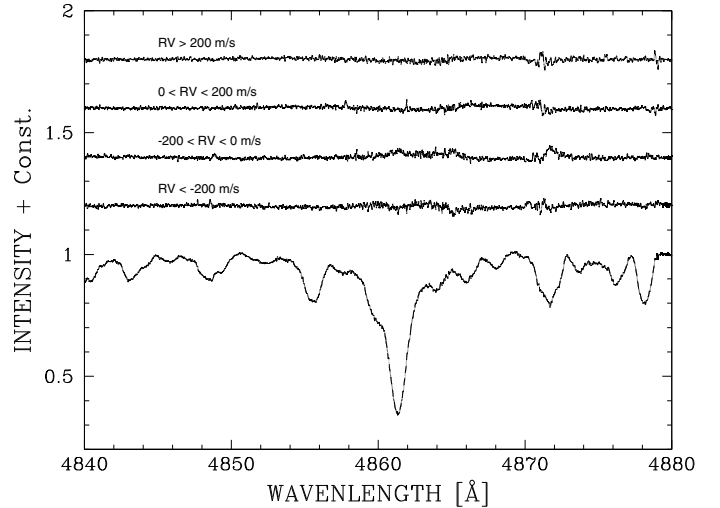


Fig. 14. Average spectrum of 30 Ari B in the $H\beta$ region. The four upper curves show the ratio of the averaged spectra in the four RV intervals ($RV < -200$ m/s , $-200 < RV < 0$ m/s , $0 < RV < 200$ m/s , and $RV > 200$ m/s) to the average spectrum in this region. There is no indication for a correlation between the RV and the depth of $H\beta$.

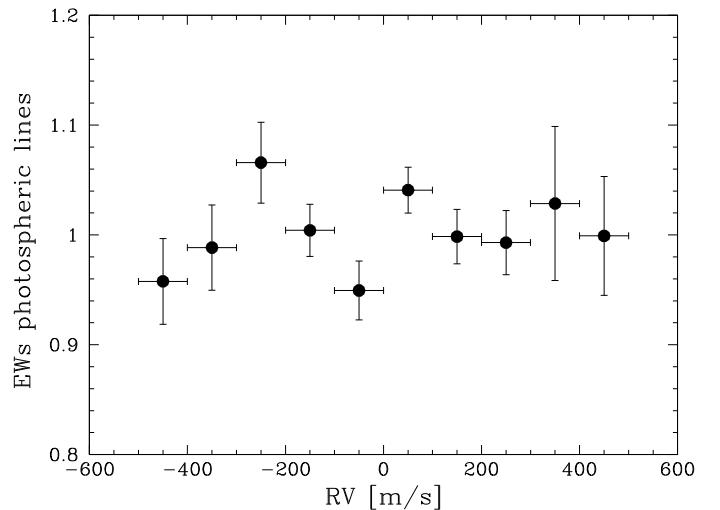


Fig. 15. Shown are measurements of the average equivalent width of photospheric lines against the RV. There is no correlation between RV and the equivalent width of the photospheric lines.

is much larger than that of γ Cep (Hatzes et al. 2003) which has a binary separation of about 40 AU. A detailed study by Desidera & Barbieri (2007) shows that the properties of planets of wide binaries (projected separation of about 200–300 AU) and orbital periods larger than 40 days are the same as that of single stars. Thus, the binary nature of 30 Ari A is presumably unimportant for 30 Ari B b.

We have measured a rotational velocity of 38.3 ± 1.8 km s^{-1} for 30 Ari B. This rotational rate implies that we most likely are viewing the star nearly equator-on. Nordström et al. (1997) measured rotational velocities of 592 early F-type stars. The median rotation rate was about 50 km s^{-1} . The average effective temperature for their sample was 6860 K which means that 30 Ari B has a slightly later spectral type than a typical member of the Nordström et al. (1997) sample. Assuming that the orbital and stellar spin axes are aligned, $\sin i$ is most likely near unity. The minimum mass derived thus is probably close to the true mass.

In any case a minimum mass of $9.88 \pm 0.94 M_{\text{Jup}}$ implies that the true mass is likely to be close to the planet/brown dwarf boundary. As pointed out by Udry & Santos (2007), while most gaseous planets have masses below $5 M_{\text{Jup}}$, the distribution has a long tail. A statistical analysis of all available data by Grether & Lineweaver (2000) shows that the driest part of the brown dwarf desert is at $M = 31^{+25}_{-18} M_{\text{Jup}}$. These authors also find that $11 \pm 3\%$ of the solar-like stars are binaries, $5 \pm 2\%$ have giant planets but less than 1% have close brown dwarf companions with orbital periods of less than 5 years. Given the fact that the inclination for most of these systems is not known, some of the suspected brown dwarf companions may even turn out to be binary stars. The only transiting object with a mass in the brown dwarf regime orbiting a star is CoRoT-Exo-3b ($M = 21.7 \pm 1.0 M_{\text{Jup}}$) (Deleuil et al. 2008). Such objects thus are rare but they do exist.

The lack of high-mass planets is particularly striking for planets with an orbital period of less than 100 days. In fact, Udry & Santos (2007) list only three planets where the mass is higher, and the orbital period is shorter than that of 30 Ari B b. According to Eggenberger et al. (2008) most of the very massive planets are in binary systems. But as pointed out above, the distance to 30 Ari A is presumably too large to have any effect on the properties of the planet.

If we compare 30 Ari B b with other extrasolar planets, then its closest match is HD 33564 b (Galland et al. 2005b): The host star also is an F6V star, $m \sin i = 9.1 M_{\text{Jup}}$, $P = 388$ days, and $e = 0.34$. 30 Ari B b thus might belong to a class of objects that is not exotic but simply represents the extension of the distribution of planets into the brown dwarf regime.

Although 30 Ari B b is the ninth planet discovered by the Tautenburg survey around a star with a mass higher than the sun, a statistically larger sample is needed before concluding that very massive planets are more common among stars more massive than the sun.

Acknowledgements. We are grateful to the user support group of the Alfred-Jensch telescope. A.P.H. and M.H. acknowledge the support from the Deutsche Forschungsgemeinschaft (DFG) of grant HA 3279/3-2, E.W.G. and F.C. of grant GU 464/11-1. M.E. acknowledges a grant by the DFG-Graduiertenkolleg 1351 “Extrasolar Planets and their Host Stars”. Additionally, D.G. acknowledges the support of a grant from the Deutschen Zentrums für Luft- und Raumfahrt (DLR) (50OW0204). This research has made use of the SIMBAD database, operated at CDS, Strasbourg, France. This publication makes use of data products from the Two Micron All Sky Survey, which is a joint project of the University of Massachusetts and the Infrared Processing and Analysis Center/California Institute of Technology, funded by the National Aeronautics and Space Administration and the National Science Foundation.

References

Allende Prieto, C., & Lambert, D. L. 1999, *A&A*, 352, 555
Boesgaard, A. M., & Friel, E. D. 1990, *ApJ*, 351, 467

Butler, R. P., Marcy, G. W., Williams, E., et al. 1996, *PASP*, 108, 500
Buzzoni, A., Chavez, M., Malagnini, M. L., et al. 2001, *PASP*, 113, 1365
Cayrel de Strobel, G., Soubiran, C., Friel, et al. 1997, *A&AS*, 124, 299
da Silva, L., Girardi, L., Pasquini, L., et al. 2006, *A&A*, 458, 609
Desidera, S., & Barbieri, M. 2007, *A&A*, 462, 345
Deleuil, M., Deeg, H. J., Alonso, R., et al. 2008, *A&A*, 491, 889
De Medeiros, J. R., Da Silva, J. R. P., & Maia, M. R. G. 2002, *ApJ*, 578, 943
Döllinger, M. P., Hatzes, A. P., Pasquini, L., et al. 2007, *A&A*, 472, 649
Döllinger, M. P., Hatzes, A. P., & Pasquini, L. 2009, *A&A*, 499, 935
Eggenberger, A., Udry, S., & Mayor, M. 2004, *A&A*, 417, 353
Endl, M., Hatzes, A. P., Cochran, W., et al. 2004, *ApJ*, 611, 112
Fortney, J. 2007, *Nature*, 449, 147
Frasca, A., Alcalá, J. M., Covino, E., et al. 2003, *A&A*, 405, 149
Frink, S., Mitchell, D. S., Quirrenbach, A., et al. 2002, *ApJ*, 576, 478
Galland, F., Lagrange, A.-M., Udry, S., et al. 2005a, *A&A*, 443, 337
Galland, F., Lagrange, A.-M., Udry, S., et al. 2005b, *A&A*, 444, L21
Galland, F., Lagrange, A.-M., Udry, S., et al. 2006, *A&A*, 452, 709
Gandolfi, D., Alcalá, J. M., Leccia, S., et al. 2008, *ApJ*, 687, 1303
Girardi, L., Bressan, A., Bertelli, G., & Chiosi, C. 2000, *A&AS*, 141, 371
Grether, D., & Lineweaver, C. H. 2006, *ApJ*, 640, 1051
Hatzes, A. P., Cochran, W. D., & Endl, M. 2003, *ApJ*, 599, 1383
Hatzes, A. P., Guenther, E. W., Endl, M., et al. 2005, *A&A*, 437, 743
Hatzes, A. P., Cochran, W. D., Endl, M., et al. 2006, *A&A*, 457, 335
Jefferys, W., Fitzpatrick, J., & McArthur, B. 1988, *Celest. Mech.*, 41, 39
König, B., Guenther, E. W., Woitas, J., & Hatzes, A. P. 2005, *A&A*, 435, 215
Kennedy, G. M., & Kenyon, S. J. 2008, *ApJ*, 673, 502
Kornet, K., Wolf, S., & Różyńska, M. 2006, *A&A*, 458, 661
Livingston, W., Wallace, L., White, O. R., & Giampapa, M. S. 2007, *ApJ*, 657, 1137
Lovis, C., & Mayor, M. 2007, *A&A*, 472, 657
Malagnini, M. L., Morossi, C., Buzzoni, A., et al. 2000, *PASP*, 112, 1455
Marsakov, V. A., & Shevelev, Yu. G. 1995, *Bull. Inf. Centre Donnees Stellaires*, 47, 13
Mermilliod, J. C. 1991, Institut d’Astronomie, Universite de Lausanne
Morbey, C. L., & Brosterhus, E. B. 1974, *PASP*, 86, 455
Nordström, B., Stefanik, R. P., & Latham, D. W. 1997, *A&AS*, 126, 21 (VizieR On-line Data Catalog: J/A=AS/126/21)
Nordström, B., Mayor, M., Andersen, J., et al. 2004, *A&A*, 418, 989
Ossendrijver, A. J. H. 1997, *A&A*, 323, 151
Pasquini, L., Döllinger, M. P., Weiss, A., et al. 2007, *A&A*, 473, 979
Perryman, M. A. C., & ESA 1997, *The Hipparcos and Tycho catalogues. Astrometric and photometric star catalogues derived from the ESA Hipparcos Space Astrometry Mission (Noordwijk, Netherlands: ESA Publications Division), ESA SP Ser.*, 1200
Pinsonneault, M. H., DePoy, D. L., & Coffee, M. 2001, *ApJ*, 556, L59
Saar, S. H., & Donahue, R. A. 1997, *ApJ*, 485, 319
Sato, B., Ando, H., & Kambe, E. 2003, *ApJ*, 597, L157
Sato, B., Izumiura, H., Toyota, E., et al. 2008, *PASJ*, 60, 539
Schuler, S. C., Kim, J. H., Tinker, M. C., Jr., et al. 2005, *ApJ*, 632, L131
Setiawan, J., Rodman, J., da Silva, L., et al. 2005, *A&A*, 437, L31
Silvotti, R., Schuh, S., Janulis, R., et al. 2007, *Nature*, 449, 189
Shatsky, N. 2001, *A&A*, 380, 238
Skrutskie, M. F., Cutri, R. M., Stiening, R., et al. 2006, *AJ*, 131, 1163
Taylor, B. J. 2003, *A&A*, 398, 721
Tolbert, C. R. 1964, *ApJ*, 139, 1105
Udry, S., & Santos, N. C. 2007, *ARA&A*, 45, 397
Valenti, J. A., Butler, R. P., & Marcy, G. W. 1995, *PASP*, 107, 966
Zickgraf, F. J., Engels, D., & Hagen, H. J. 2003, *A&A*, 406, 535
Zombeck, M. V., *Handbook of Astronomy and Astrophysics*, 3rd edition (Cambridge, UK: Cambridge University Press)